

PREPARED FOR SUBMISSION TO JHEP

Chiral phase transition of QCD with $N_f = 2 + 1$ flavors from holography

Danning Li,^a Mei Huang^{b,c}

^a*Department of Physics, Jinan University, Guangzhou 510632, P.R. China*

^b*Institute of High Energy Physics, Chinese Academy of Sciences, Beijing 100049, P.R. China*

^c*Theoretical Physics Center for Science Facilities, Chinese Academy of Sciences, Beijing 100049, P.R. China*

E-mail: lidanning@jnu.edu.cn, huangm@ihep.ac.cn

ABSTRACT: Chiral phase transition for three-flavor $N_f = 2 + 1$ QCD with $m_u = m_d \neq m_s$ is investigated in a modified soft-wall holographic QCD model. Solving temperature dependent chiral condensates from equations of motion of the modified soft-wall model, we extract the quark mass dependence of the order of chiral phase transition in the case of $N_f = 2 + 1$, and the result is in agreement with the “Colombia Plot”, which is summarized from lattice simulations and other non-perturbative methods. First order phase transition is observed around the three flavor chiral limit $m_{u/d} = 0, m_s = 0$, while at sufficient large quark masses it turns to be a crossover phase transition. The first order and crossover regions are separated by a second order phase transition line. The second order line is divided into two parts by the $m_{u/d} = m_s$ line, and the m_s dependence of the transition temperature in these two parts are totally contrast, which might indicate that the two parts are governed by different universality classes.

KEYWORDS: Chiral phase transition, chiral condensate, soft-wall AdS/QCD

Contents

1	Introduction	1
2	Soft-wall model in $N_f = 2 + 1$ case	3
2.1	Background	3
2.2	Boundary condition and numerical solutions	6
3	Chiral condensate and phase diagram in mass plane	8
4	Conclusion and discussion	12

1 Introduction

Quantum Chromodynamics(QCD) is widely accepted as the fundamental theory of strong interactions, and QCD vacuum is characterized by spontaneous chiral symmetry breaking together with color charge confinement. The dynamically generated chiral condensate $\langle\bar{\psi}\psi\rangle$ in the vacuum serves as quarks' dynamical mass and spontaneously breaks the chiral symmetry, which is an exact symmetry of QCD lagrangian when quarks are massless. It is believed that at sufficient high temperature and/or density, quark condensate might be destroyed completely and the spontaneous breaking symmetry would be restored. Understanding the property of chiral phase transition has been an important topic in both non-perturbative QCD and cosmology for decades[1].

The order of chiral phase transition depends sensitively on the inertial degrees of freedom of the system, such as the number of flavors(N_f) and the mass of quarks(m_u, m_d and m_s). Based on theoretical consideration and lattice QCD simulations [2–4], the expected three flavor phase diagram in the quark mass plane, describing quark mass dependence of the order of QCD phase transitions, is summarized in the sketch plot (it is also called “Columbia Plot”) shown in Fig.1(a). In this sketch plot, the whole $m_{u/d} - m_s$ plane are divided into three simply connected region: two first order zones in the bottom left corner and the upper right corner as well as the crossover region in the middle. The upper right corner is near the infinite quark mass limit $m_u = m_d = m_s = \infty$, where the breaking and restoration of Z_3 centre symmetry, related to confinement/deconfinement phase transition, are well defined. The bottom left corner is near the chiral limit $m_u = m_d = m_s = 0$, where the breaking and restoration of chiral symmetry, related to chiral phase transition, are well defined. In between these two regions, there are no known exact symmetries and the phase transitions are expected to be a continual and rapid transition between different phases, usually named “crossover”. The boundary of these three regions are second order lines, where the phase transitions are expected to be of second order. Furthermore, we noted

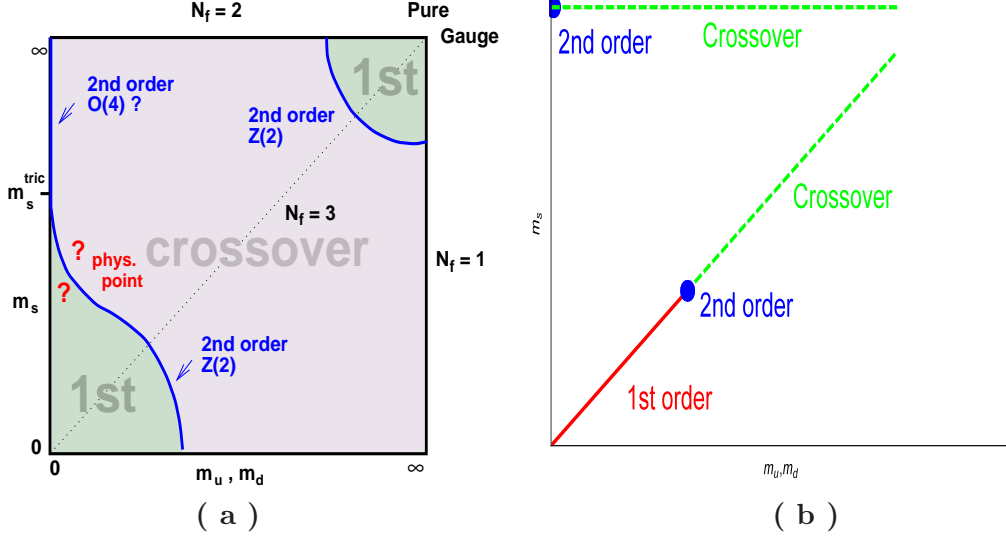


Figure 1. Panel.(a) shows the “Colombia Plot” which gives expected phase diagram in the quark masses $m_u = m_d, m_s$ plane (Taken from [2]). Panel.(b) gives the prediction of the mass diagram of $N_f = 2$ and $N_f = 3$ in a modified soft-wall model(Taken from [5]).

that the second order line between the bottom left first order region and the crossover region is divided by the $SU(3)$ diagonal line with $m_u = m_d = m_s$ into two parts, the upper one of which is expected to be governed by the $O(4)$ universality class[6] while the lower one of which is expected to be governed by the $Z(2)$ universality class.

Theoretically, the dynamics of QCD near phase transition is non-perturbative, and normal perturbative methods of quantum field theory become invalid here. Lattice QCD has been considered as the most reliable non-perturbative method to study non-perturbative properties of QCD. However, lattice QCD simulations still require further improvements in several aspects, especially the difficulty called sign problem at finite chemical potential, which is waited to be solved in order to extract full understanding on QCD phase diagram. Hence, it is quite necessary to develop other non-perturbative methods. The recent progress of anti-de Sitter/conformal field theory (AdS/CFT) correspondence and the conjecture of the gravity/gauge duality[7–9] does provide such a new powerful tool to tackle the strong coupling problem of gauge theory like QCD.

In the framework of holography, by breaking the conformal symmetry of the original AdS/CFT correspondence in different ways, efforts towards realistic holographical description of non-perturbative physics of QCD, such as hadron physics[10–34] and hot/dense QCD matter[35–50], have been made both in top-down approaches and in bottom-up approaches(see Refs.[51–55] for reviews). Different from top-down approach, bottom-up holographic QCD starts from QCD phenomena and try to build up more realistic holographic models. In this approach, chiral phase transition has been studied in several different models [5, 56–65]. Most of these studies considered the case with equal quark masses for all quarks. As can be seen from Fig.1(a), it is also interesting to consider the cases when $m_{u/d} \neq m_s$, where the physical point locates. In our previous studies[5, 63],

based on soft-wall AdS/QCD model [11], the mass dependence of chiral phase transition is extracted, as shown in Fig.1(b). The qualitative results for $SU(2)$ and $SU(3)$ cases are in good agreement with the current understanding from Fig.1(a): for two flavor case it starts from a second order phase transition and turns to be crossover at any finite quark mass while for three flavor case it starts from a first order phase transition and only at sufficient large quark masses it turns to be crossover. Furthermore, in [65], we extend these studies to finite magnetic field, and find that it can provide good description on inverse magnetic catalysis effect, which was discovered in lattice QCD[66, 67] and studied in other methods[68–78] recently. However, the cases when $m_{u/d} \neq m_s$ have not been examined in this model. Therefore, in this work, we will extend our studies in [5, 63] to $N_f = 2 + 1$ when $m_l \equiv m_u = m_d \neq m_s$ and study the property of chiral phase transition.

The paper is organized as follows. In Sec.2, we give a short introduction on the model and the numerical method we used, especially on how to introduce quark masses and chiral condensates in the model. Then in Sec.3 we show numerical results from our model study, especially the quark mass dependence of the order of the chiral phase transition like Fig.1. Finally in Sec.4 a brief discussion will be given.

2 Soft-wall model in $N_f = 2 + 1$ case

2.1 Background

In the original paper of soft-wall model [11], the 4D global chiral symmetry $SU(N_f)_L \times SU(N_f)_R$ is promoted to 5D and becomes local gauge symmetry of the following action

$$S = - \int d^5x \sqrt{-g} e^{-\Phi} \text{Tr}(D_m X^\dagger D^m X + V_X(X) + \frac{1}{4g_5^2}(F_L^2 + F_R^2)), \quad (2.1)$$

with Φ the dilaton field, X a complex scalar field, V_X the scalar potential, F_{mn} the field strength defined as $F_{mn}^{L/R} = \partial_m A_n^{L/R} - \partial_n A_m^{L/R} - i[A_m^{L/R}, A_n^{L/R}]$ in terms of the left/right hand gauge potential $A^{L/R}$, g_5 the gauge coupling, g the determinant of metric g_{mn} , and the covariant derivative D_m defined as $D_m X = \partial_m X - iA_m^L X + iX A_m^R$. The scalar potential V_X only takes the mass term and has the form of

$$V_X(X) = M_5^2 X^\dagger X. \quad (2.2)$$

From the AdS/CFT prescription $M_5^2 = (\Delta - p)(\Delta + p - 4)$ [9], the mass of the complex scalar field X M_5^2 can be determined as $M_5^2 = \frac{3}{L^2}$ (we will take the AdS radius $L = 1$ in this work) by taking $\Delta = 3, p = 0$. The dilaton field is taken to be a simple quadratic form $\Phi(z) = \mu^2 z^2$. In this way, the meson spectra are shown to be linear with respect to the radial excitation quantum number n at large n , which gives good description of the linear behavior of meson spectra. However, in the original soft-wall model, there is no spontaneous chiral symmetry breaking in QCD vacuum and also no restoration at sufficient high temperature.

As pointed out in [5, 63], further modifications of the dilaton field and the scalar potential are necessary in order to describe the spontaneous chiral symmetry breaking in

QCD vacuum and its restoration. The specific profile of the dilaton field are proposed [5, 63] and it takes the following form

$$\Phi(z) = -\mu_1^2 z^2 + (\mu_1^2 + \mu_0^2) z^2 \tanh(\mu_2^2 z^2), \quad (2.3)$$

which tends to be pure negative quadratic $\Phi(z) \simeq -\mu_1^2 z^2 + o(z^2)$ in ultraviolet(UV) region $z \rightarrow 0$ and positive quadratic form $\Phi(z) \simeq \mu_1^2 z^2$ in the infrared(IR) region $z \rightarrow \infty$. The positive quadratic behavior of $\Phi(z)$ is responsible for the linear spectra, which is well known in the soft-wall AdS/QCD. The scalar potential takes the first several leading powers of V_X and has the form of

$$V_X(X) = M_5^2 X^\dagger X + \lambda |X|^4 + \gamma \text{Re}[\det(X)]. \quad (2.4)$$

In [5, 63], we have shown that the negative part as well as the quartic term $\lambda |X|^4$ in the scalar potential are essential for the spontaneous chiral symmetry breaking in the vacuum as well as its restoration at sufficient high temperature. In $SU(2)$ or two-flavor case, the t'Hooft determinant term $\gamma \text{Re}[\det(X)]$ is taken to be zero, and we find a second order phase transition in the chiral limit and a crossover transition at any finite quark mass case. In $SU(3)$ or three-flavor case, we consider the t'Hooft limit, and we find a first order chiral phase transition in the chiral limit, while only at sufficient quark mass the phase transition turns to be a crossover one. Furthermore, in our recent study [65], we show that after introducing magnetic field through the Einstein-Maxwell sector, the above $SU(2)$ model can describe inverse magnetic catalysis in the soft-wall model quite well. All the qualitative results are in agreement with the current understanding from lattice simulations[2–4, 66, 67] and other non-perturbative studies.

Nevertheless, in our previous study, we have only considered equal mass in both the $SU(2)$ and $SU(3)$ cases, i.e., $m_u = m_d$ and $m_u = m_d = m_s$. Therefore, we can only obtain the top line and the diagonal line in Fig.1. As shown in Fig.1, it is also interesting to consider the case $N_f = 2 + 1$ with $m_l \equiv m_u = m_d \neq m_s$ case. It would be a quite natural extension of our previous study in $SU(3)$ case to the $N_f = 2 + 1$ case. In the following, A_L, A_R will be set to be zero, since only the scalar field X is relevant for the chiral phase transition. Since $m_l \equiv m_u = m_d \neq m_s$, the complex scalar field should take the following form

$$X = \begin{pmatrix} \frac{\chi_l(z)}{\sqrt{2}} & 0 & 0 \\ 0 & \frac{\chi_l(z)}{\sqrt{2}} & 0 \\ 0 & 0 & \frac{\chi_s(z)}{\sqrt{2}} \end{pmatrix}, \quad (2.5)$$

instead of a simple χI_3 with I_3 the 3×3 matrix. Here, we assume that $\chi_l(z), \chi_s(z)$ are functions of the 5D coordinate z only and the factor $\frac{1}{\sqrt{2}}$ is just a normalization constant¹. When $m_l \neq m_s$, we should have $\chi_l \neq \chi_s$, since the boundary values of χ_l, χ_s are related to the quark masses. Under this ansatz, we can get the effective form of the action Eq.2.1 as

¹We set this factor to make sure the coefficients of kinetic terms of χ_u, χ_d, χ_s are $\frac{1}{2}$.

following

$$S[\chi_l, \chi_s] = - \int d^5x \sqrt{-g} e^{-\Phi} \left\{ g^{zz} (\chi_l'^2 + \frac{1}{2} \chi_s'^2) + \frac{1}{L^2} \left[-3(\chi_l^2 + \frac{1}{2} \chi_s^2) + v_4(2\chi_l^4 + \chi_s^4) + 3v_3\chi_l^2\chi_s^2 \right] \right\}, \quad (2.6)$$

with $v_3 = \frac{2\sqrt{2}}{3}\gamma$, $v_4 = \frac{\lambda}{4}$ and L the AdS radius, which will not affect the final results and will be taken to be 1 later.

As in [5, 63], we will neglect the back-reaction of χ_l, χ_s to the background metric, and take the simple AdS-Schwarzschild(AdS-SW) black hole solutions

$$dS^2 = e^{2A_s(z)} (-f(z)dt^2 + \frac{1}{f(z)}dz^2 + dx_i dx^i), \quad (2.7)$$

$$A_s(z) = -\log(z), \quad (2.8)$$

$$f(z) = 1 - \frac{z^4}{z_h^4}, \quad (2.9)$$

where z_h is the black hole horizon defined at $f(z_h) = 0$ and could be related to the temperature T by the following relation

$$T = |\frac{f'(z_h)}{4\pi}| = \frac{1}{\pi z_h}. \quad (2.10)$$

Under this ansatz, the equations of motion for χ_l, χ_s could be derived as the following form

$$\chi_l'' + (3A_s' - \Phi' + \frac{f'}{f})\chi_l' + \frac{e^{2A_s}}{f}(3\chi_l - 3v_3\chi_l\chi_s - 4v_4\chi_l^3) = 0, \quad (2.11)$$

$$\chi_s'' + (3A_s' - \Phi' + \frac{f'}{f})\chi_s' + \frac{e^{2A_s}}{f}(3\chi_s - 3v_3\chi_l^2 - 4v_4\chi_s^3) = 0. \quad (2.12)$$

Please notice that in the $SU(3)$ case with equal quark mass $m_l(\equiv m_u = m_d) = m_s$, we can have $\chi_l = \chi_s \equiv \chi$, and the above two equations will be reduced to the same one

$$\chi'' + (3A_s' - \Phi' + \frac{f'}{f})\chi' + \frac{e^{2A_s}}{f}(3\chi - 3v_3\chi^2 - 4v_4\chi^3) = 0, \quad (2.13)$$

which is exactly the same as the one in [5, 63]. In [5, 63], we have taken $v_3 = -3, v_4 = 8$ to show the qualitative behavior of chiral phase transition in this model. Therefore, in this work we will continue to use this group of parameters.

The dilaton profile Eq.2.3 has been shown to give well description of both chiral symmetry breaking and linear confinement. Thus in this work we will stick to this profile and extend the model to $m_l \neq m_s$ case. The parameters μ_0, μ_1, μ_2 in the dilaton profile Eq.(2.3) will be taken as the same value

$$\mu_0 = 0.43\text{GeV}, \mu_1 = 0.83\text{GeV}, \mu_2 = 0.176\text{GeV} \quad (2.14)$$

as in [5, 63]. In the next section, we will show how to solve the order parameter of chiral phase transition from this model.

2.2 Boundary condition and numerical solutions

Under the background Eqs.(2.3,2.7,2.8,2.9), the equations of motion for χ_l, χ_s could be solved numerically. Before that, we should specify the boundary condition.

Firstly, near the Ultraviolet (UV) boundary $z = 0$, one can extract the perturbative expansion solution of χ_l, χ_s as

$$\chi_l = c_l z - 3c_l c_s v_3 z^2 - (\mu_1^2 - 2c_l^2 v_4 + \frac{9}{2}c_s^2 v_3^2 + \frac{9}{2}c_l^2 v_3^2)c_l z^3 \log(z) + d_l z^3 + \dots, \quad (2.15)$$

$$\chi_s = c_s z - 3c_l^2 v_3 z^2 - (\mu_1^2 - 2c_s^2 v_4 - 9c_l^2 v_3^2)c_s z^3 \log(z) + d_s z^3 + \dots, \quad (2.16)$$

with c_l, d_l, c_s, d_s four integral constants of the two coupled second order ordinary derivative equations Eqs.(2.11,2.12), which could be related to the current quark masses m_l, m_s and chiral condensates $\sigma_l \equiv \langle \bar{u}u \rangle = \langle \bar{d}d \rangle, \sigma_s \equiv \langle \bar{s}s \rangle$ by the following equations[11, 79]

$$c_l = m_l \zeta, \quad (2.17)$$

$$d_l = \frac{\sigma_l}{\zeta}, \quad (2.18)$$

$$c_s = m_s \zeta, \quad (2.19)$$

$$d_s = \frac{\sigma_s}{\zeta}, \quad (2.20)$$

and $\zeta = \frac{\sqrt{3}}{2\pi}$. As mentioned above, in this work we will try to study chiral phase transition under different values of m_l, m_s , so we will tune m_l, m_s in the later calculation. At a first sight, the other two integral constants σ_l, σ_s could be chosen independently on m_l, m_s . However, if one checks the two equations of motion Eqs.(2.11,2.12), there are terms like

$$\frac{f' \chi_l' + e^{2A_s}(3\chi_l - v_3 \chi_l \chi_s - v_4 \chi_l^3)}{f(z)}, \quad (2.21)$$

$$\frac{f' \chi_s' + e^{2A_s}(3\chi_s - v_3 \chi_l^2 - v_4 \chi_s^3)}{f(z)}, \quad (2.22)$$

with $f(z)$ in the denominator. At the horizon $z = z_h$, we have $f(z_h) = 0$. Thus, z_h is an apparent singularity of Eqs.(2.11,2.12), where χ_l, χ_s might be divergent. To avoid this divergence, physical solutions of χ_l, χ_s should also satisfy the infrared (IR) boundary conditions

$$Q_l(z_h) \equiv f' \chi_l' + e^{2A_s}(3\chi_l - v_3 \chi_l \chi_s - v_4 \chi_l^3)|_{z=z_h} = 0, \quad (2.23)$$

$$Q_s(z_h) \equiv f' \chi_s' + e^{2A_s}(3\chi_s - v_3 \chi_l^2 - v_4 \chi_s^3)|_{z=z_h} = 0, \quad (2.24)$$

to cancel the singularity at the horizon where $f(z_h) = 0$. It is easy to understand that with these two additional conditions from the requirement of the regularity of χ_l, χ_s , the other two UV coefficients σ_l, σ_s cannot be considered as free integral constants with given m_l, m_s . Instead, they should be solved from the equations of motion.

Therefore, to find a physical solution with given m_l, m_s , one has to solve the boundary value problem

$$\begin{aligned} \lim_{\epsilon \rightarrow 0} \frac{\chi_l(\epsilon)}{\epsilon} &= m_l \zeta, \quad \lim_{\epsilon \rightarrow 0} \frac{\chi_s(\epsilon)}{\epsilon} = m_s \zeta, \\ Q_l(z_h) &= 0, \quad Q_s(z_h) = 0. \end{aligned} \quad (2.25)$$

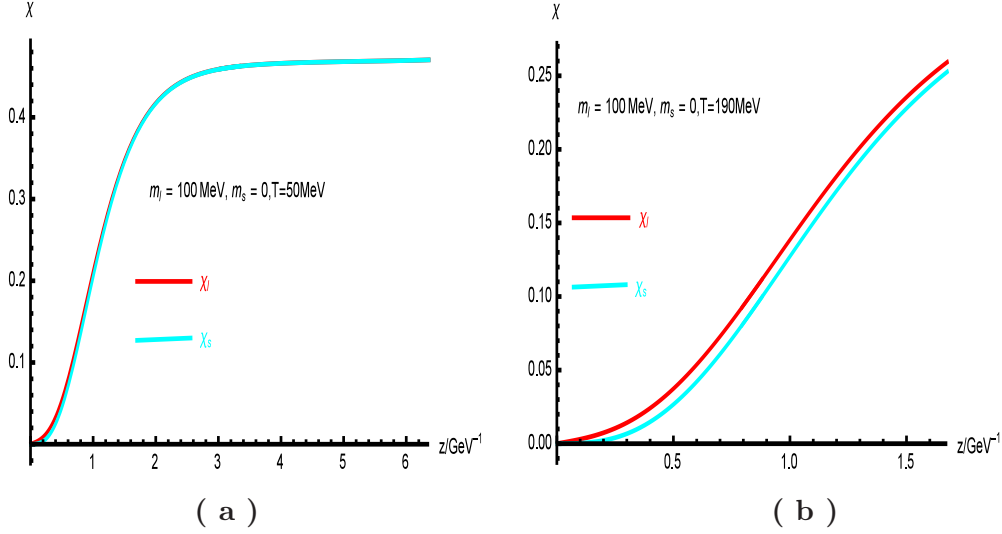


Figure 2. Solutions of χ_l and χ_s as functions of z when $m_l = 100\text{MeV}$, $m_s = 0$. Panel(a) shows the low temperature solutions with $T = 50\text{MeV}$ and Panel(b) shows the behavior for $T = 190\text{MeV}$. At low temperature, χ_l and χ_s are almost the same while at higher temperature they would be separated.

One can use the “Shooting Method” to solve this boundary value problem. After it was solved, one can extract the chiral condensates σ_l and σ_s . As an example, we take $m_l = 100\text{MeV}$, $m_s = 0$, $T = 50\text{MeV}$, $z_h = \frac{1}{\pi T} \approx 6.37\text{GeV}^{-1}$ and $T = 190\text{MeV}$, $z_h = \frac{1}{\pi T} \approx 1.67\text{GeV}^{-1}$. For $T = 50\text{MeV}$, $z_h = \frac{1}{\pi T} \approx 6.37\text{GeV}^{-1}$, we get $\sigma_l = 0.10\text{GeV}^3 \approx (470\text{MeV})^3$, $\sigma_s = 0.12\text{GeV}^3 \approx (495\text{MeV})^3$ using “Shooting Method” and plot the corresponding regular χ_l, χ_s solutions in Fig.2(a). The non-vanishing values of σ_l, σ_s at low temperature are signal of chiral symmetry breaking of the vacuum. From the figure, we could see that, at small z , χ_l, χ_s are slightly separated from each other, since the leading terms in this region are $m_l \zeta z$ and $m_s \zeta z$, which are different when $m_l \neq m_s$. In the IR region when z is large, χ_l, χ_s is almost overlap and approach a constant value $\chi_l^h \equiv \chi_l(z_h) \approx \chi_s^h \equiv \chi_s(z_h) \approx 0.47$. Like in $m_l = m_s$ case, the UV region of the solutions are governed by the trivial vacuum $\chi_l = \chi_s = 0$ while the IR region are governed by the non-trivial vacuum $\chi_l \neq 0, \chi_s \neq 0$.

Then at temperature up to $T = 190\text{MeV}$, we get $\sigma_l = 0.06\text{GeV}^3 \approx (389\text{MeV})^3$, $\sigma_s = 0.07\text{GeV}^3 \approx (412\text{MeV})^3$, which are smaller than the corresponding values at $T = 50\text{MeV}$, showing that chiral condensate are partly destroyed by temperature. In Fig.2(b) we plot the solutions of χ_l, χ_s at temperature $T = 190\text{MeV}$. From the figure, we could see that at high temperature, χ_l, χ_s are still interpolation of the trivial vacuum and non-zero horizon values χ_l^h, χ_s^h . The separation of χ_l, χ_s become larger than that at low temperature.

As a short summary, we have shown that the regular condition of χ_l, χ_s would require the condensates σ_l, σ_s as functions of quark masses m_l, m_s and temperature T . Since chiral condensates are the order parameters of chiral phase transition, we will work out the quark mass and temperature dependence of σ_l, σ_s to extract the information of chiral

phase transition in next section.

3 Chiral condensate and phase diagram in mass plane

As mentioned in the introduction, it is also interesting to consider the property of chiral phase transition when $m_l \neq m_s$. In Sec.2.2 we have shown that in the extended $N_f = 2 + 1$ model one can solve chiral condensates σ_l, σ_s from the equations of motion Eqs.(2.11,2.12) with given quark masses m_l, m_s and the temperature T . Hence, in this section we will try to extract the quark masses and temperature dependence of chiral condensates, which contains the information of chiral phase transition.

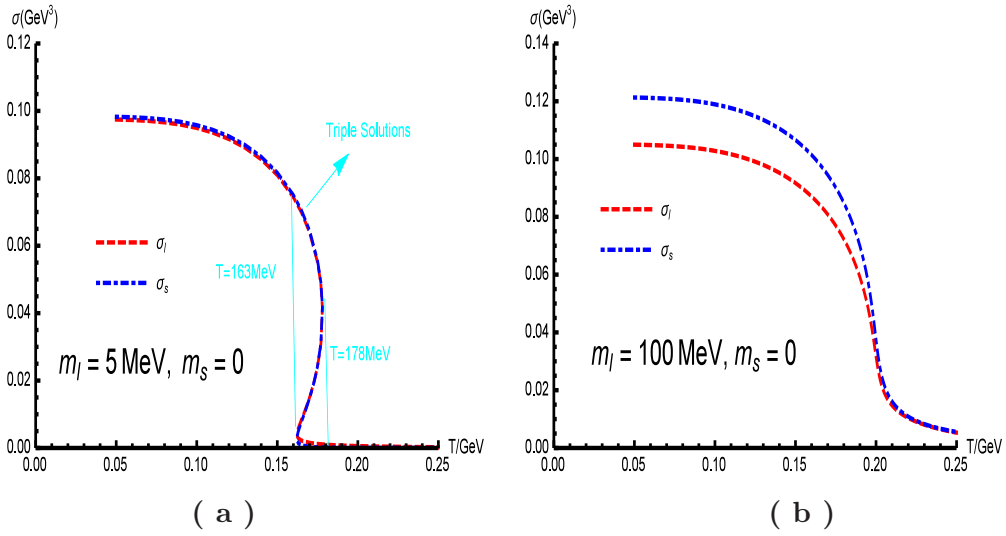


Figure 3. Chiral condensates σ_l, σ_s as functions of temperature T . In Panel.(a), σ_l, σ_s for $m_l = 5 \text{ MeV}, m_s = 0$ are given. Below $T = 163 \text{ MeV}$ and above $T = 178 \text{ MeV}$, both σ_l and σ_s decrease monotonically with temperature T , while between $T = 163 \text{ MeV}$ and $T = 178 \text{ MeV}$ they are triple-value functions of T , showing a kind of characteristic behavior of first order phase transition. In Panel.(b), the behavior of $\sigma_{l,s}$ for $m_l = 100 \text{ MeV}, m_s = 0$ are given. A kind of monotonically decreasing in the whole temperature region are shown, which shows a characteristic behavior of crossover transition.

Firstly, we take $m_s = 0$ and $m_l = 5 \text{ MeV}$. Using “Shooting Method”, we solve σ_l, σ_s from Eqs.(2.11,2.12). The results are shown in Fig.3(a). From the figure, we could see that since $m_l = 5 \text{ MeV} \simeq m_s = 0$, the differences of σ_l and σ_s are not very large. At low temperature, below 100 MeV , both σ_l and σ_s are almost constants 0.1 GeV^3 , showing the breaking of chiral symmetry in the vacuum. At high temperature, above 185 MeV , σ_l and σ_s decrease to number smaller than 0.001 GeV^3 . As we showed in [5], the non-zero value of the high temperature tail comes from the non-zero quark masses other than spontaneous chiral symmetry breaking, since in the chiral limit, this tail will tend to be zero. Therefore, in fact the high temperature tail stands for the symmetry restoration phase. So from the

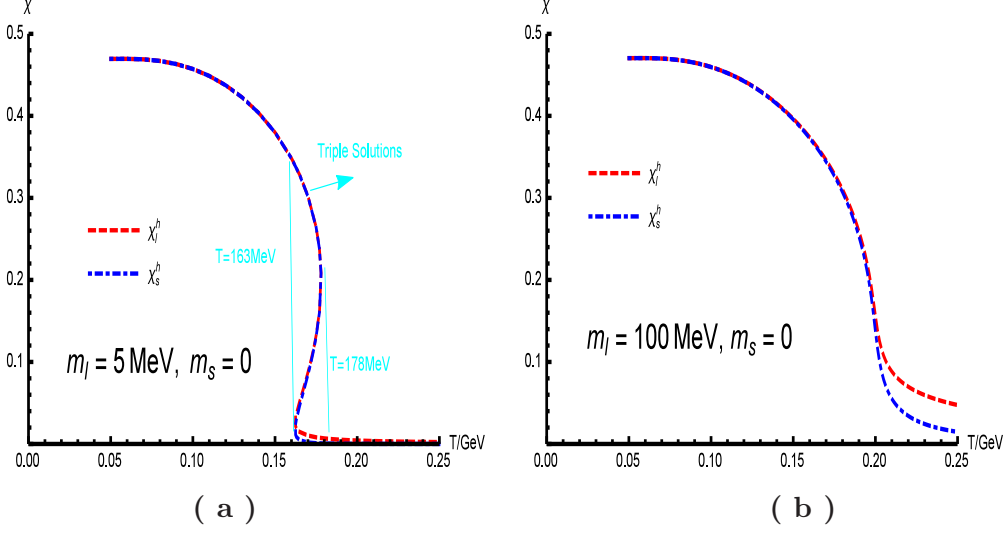


Figure 4. The near horizon boundary value χ_l^h, χ_s^h as functions of temperature T . Panel.(a) and Panel.(b) give the result for $m_l = 5\text{MeV}, m_s = 0$ and $m_l = 100\text{MeV}, m_s = 0$ respectively. At low temperature, χ_l and χ_s are almost the same while above transition point they are separated.

numerical results in Fig.3(a), we see a low temperature symmetry breaking phase and a high temperature symmetry restoration phase, which indicates a phase transition. Then, we look into the intermediate temperature region and found that within $163\text{MeV} < T < 178\text{MeV}$ there are three branches of solutions at the same temperature. As discussed in [5], this kind of behavior is a characteristic signal of first order phase transition. The exact transition temperature would be located inside the temperature region $163\text{MeV} < T < 178\text{MeV}$ and can be worked out from the free energy. However, here we will focus on the order of the transition other than the critical temperature, so we would not try to extract the exact transition temperature for the first order transition. Furthermore, we also plot the temperature dependence of the horizon value $\chi_l^h \equiv \chi_s(z_h), \chi_s^h \equiv \chi_s(z_h)$ in Fig.4(a). There, we can see the same behavior as Fig.3(a). At small temperature, χ_l, χ_s are dominant by the non-trivial vacuum of scalar potential, while at high temperature they are dominant by the trivial $\chi_l = 0, \chi_s = 0$ vacuum.

Then, we increase m_l to $m_l = 100\text{MeV}$ while keeping $m_s = 0$. After solving the equations of motion, the results of chiral condensates σ_l, σ_s and χ_l^h, χ_s^h are given in Fig.3(b) and 4(b), respectively. There we could see that at low temperature, both σ_l and σ_s increase with the increasing of m_l . Below $T = 120\text{MeV}$, σ_l and σ_s are almost constants $\sigma_l \approx 0.11\text{GeV}^3, \sigma_s \approx 0.12\text{GeV}^3$. It is also easy to see that σ_s increase faster than σ_l . As a result, the separation of σ_l and σ_s becomes larger than that at $m_l = 5\text{MeV}, m_s = 0$. At high temperature, again we could see that σ_l, σ_s decrease to a very small value, showing the restoration of the spontaneous breaking symmetry (though explicit breaking is always there due to the non-zero quark masses). However, different from $m_l = 5\text{MeV}$ case, in this case σ_l and σ_s decrease monotonically from the vacuum expectation values to zero without the triple branches region. Furthermore, at around $T = 200\text{MeV}$, σ_l and σ_s decrease very fast

from the value at symmetry breaking phase to the value at symmetry restoration phase. This kind of behavior shows a characteristic crossover phase transition. As for χ_l^h, χ_s^h , we see that they also decrease monotonically from a larger value to zero. But differently, at low temperature, χ_l^h, χ_s^h do not change much with the increasing of m_l . The low temperature value of these two quantities are still around 0.47. At high temperature, they monotonically decrease to zero at different rate. From the figure, we could see that χ_l^h decreases faster than χ_s^h .

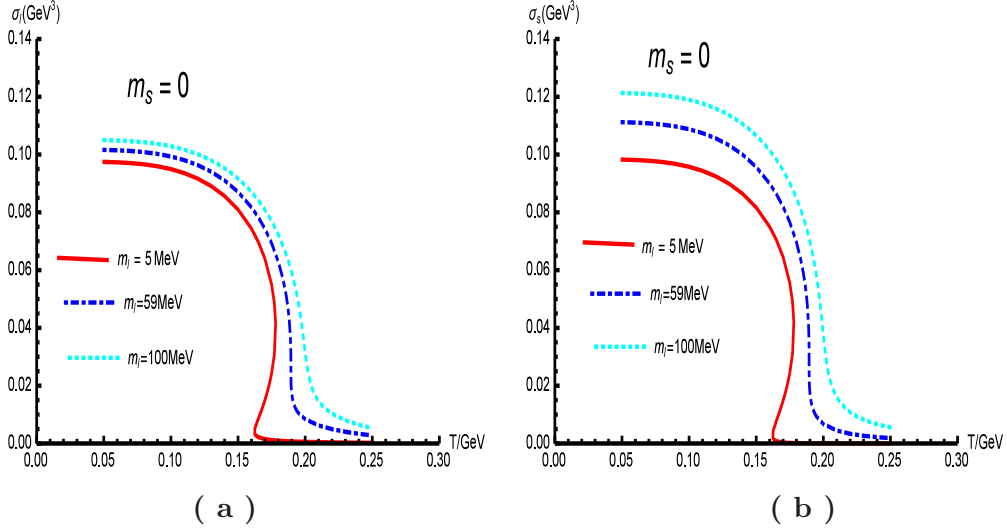


Figure 5. Panel.(a) shows the behavior of σ_l as a function of temperature T for different m_l when $m_s = 0$. Panel.(b) shows the behavior of σ_s as a function of temperature T for different m_l when $m_s = 0$. From Panel.(a,b), one can expect that when $m_s = 0$ at small m_l region the phase transition is of first order kind, while at sufficient high T it turns to be a crossover one. The critical case happens when $m_l \approx 59\text{MeV}$, where $\frac{d\sigma}{dT}$ would diverge at around $T = 189.3\text{MeV}$ for both σ_l and σ_s , showing a kind of second order phase transition.

From the above discussion, it seems that when $m_s = 0$, at small m_l the system undergoes first order phase transition while at large m_l the phase transition turns to be crossover. To be more rigorous, we fix $m_s = 0$ and scan m_l . From Fig.5, we find that when m_l is smaller than 59MeV, both σ_l, σ_s are non-monotonic, indicating a first order phase transition. Then the non-monotonic region shrinks as the increasing of m_l . At the critical value $m_l = 59\text{MeV}$, the triple branches region disappears. At this value, we found that both the derivatives of $\sigma_l(T), \sigma_s(T)$ with respect to temperature T diverge at the same temperature $T = 189.3\text{MeV}$, which reveals a second order phase transition. Then, above $m_l = 59\text{MeV}$, we find that σ_l and σ_s decreases monotonically from nonzero value to zero, showing a crossover phase transition.

Then we increase m_s to $m_s = 200\text{MeV}$ and scan m_l . We plot the results of σ_l, σ_s in Fig.6. We see that qualitatively the results are similar to those when $m_s = 0$. When temperature increases, condensates would decrease from nonzero value to zero. When

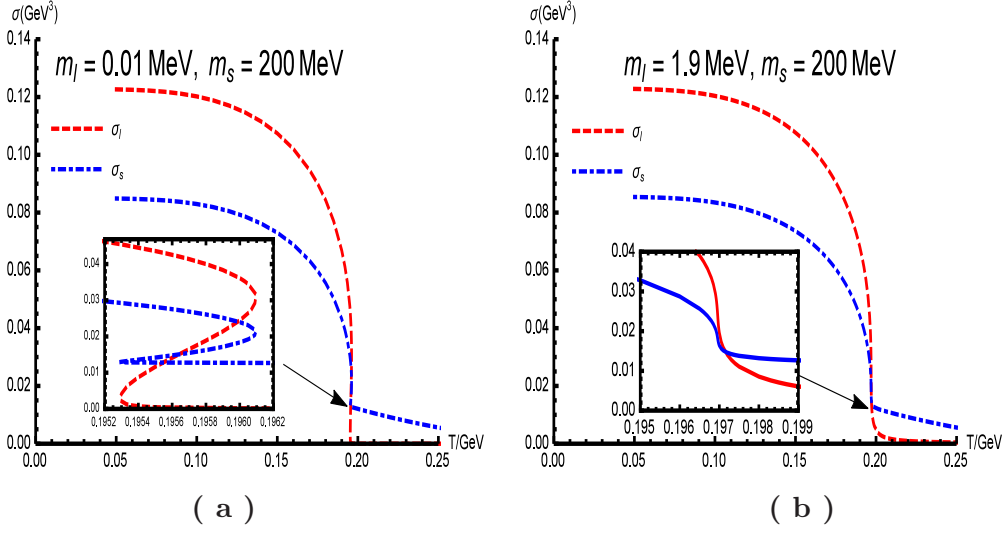


Figure 6. Panel.(a) shows the behavior of σ_l as a function of temperature T for different m_l when $m_s = 200 \text{ MeV}$. Panel.(b) shows the behavior of σ_s as a function of temperature T for different m_l when $m_s = 200 \text{ MeV}$. From Panel.(a,b), one can expect that when $m_s = 200 \text{ MeV}$ at small m_l region the phase transition is of first order kind, while at sufficient high T it turns to be a crossover one. The critical case happens when $m_l \approx 1.9 \text{ MeV}$, where $\frac{d\sigma}{dT}$ would diverge at around $T = 196.9 \text{ MeV}$ for both σ_l and σ_s , showing a kind of second order phase transition.

$m_l = 0.01 \text{ MeV}$, there is a short region where σ_l, σ_s have triple branches. But the triple solutions region becomes very short (from $T \approx 195.3 \text{ MeV}$ to $T \approx 196.1 \text{ MeV}$) comparing to $m_s = 0$ case. Then at larger m_l the behavior becomes crossover. The critical value of m_l is around 1.9 MeV and from Fig.6(b) the second order transition temperature becomes 196.9 MeV .

Furthermore, we tune m_s from 0 to 200 MeV . We find that for each value of m_s , there is a critical m_l , at which chiral phase transition becomes second order. Here we note that both at large m_s and small m_s , the triple solutions region of σ_l, σ_s disappears at the same critical mass m_l^c and $\frac{d\sigma}{dT}$ diverges at the same critical temperature for both σ_l and σ_s . Below this critical m_l^c , the transition is of first order while above it the phase transition is crossover. We plot the critical line in Fig.7(a). From the figure, we see that the critical line divides the whole plane into two parts: the bottom left part is first order phase transition region while the upper right part is crossover transition region. Qualitatively, this result is in agreement with the “Colombia Plot” in Fig.1(a), which is summarized from lattice simulations and other effective methods. Moreover, from the critical line, one can extract the exact transition temperature, where $\frac{d\sigma}{dT}$ diverges for both σ_l and σ_s . The results are given in Panel.(b). There one can read that the transition temperature of the second order phase transition decreases when it approaches $m_l = m_s \approx 0.037 \text{ GeV}$ from left, while it increases when from right. This might indicate that the two branches of the critical line separated by the $m_l = m_s$ point might be governed by different universality classes, though

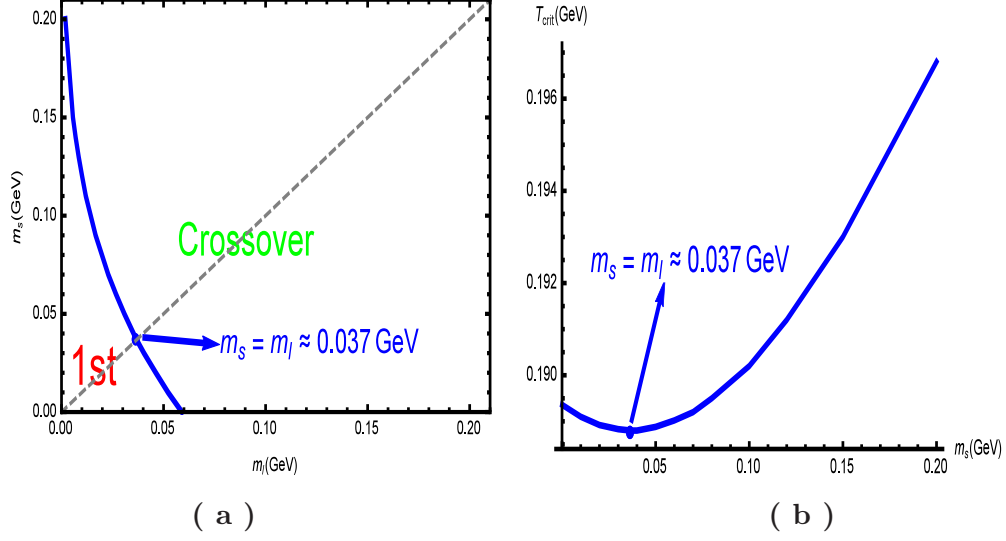


Figure 7. The phase diagram for chiral phase transition in $m_l - m_s$ plane. The blue solid line in Panel.(a) shows the critical line(second order line) between the first order region(the bottom left corner) and the crossover region(the upper right corner). In Panel.(b), the temperature for the critical line in Panel.(a) are given. The blue dot in Panel.(a)(b) are $m_s = m_l = 0.037\text{ GeV}$, the critical masses when $m_l = m_s$, which is the same as the one we extracted in $SU(3)$ case in [5]. In Panel.(b), in the left branch to the blue dot, the transition temperature of the critical line decreases with the increasing of m_s , while in the right branch it increases, indicating that the two branches might be governed by different universality classes.

the exact correspondence is out of the scope of this work. Roughly speaking, this is also consistent with Fig.1(a), where the upper part of the critical line is governed by $O(4)$ classes and the bottom part is governed by $Z(2)$ classes.

4 Conclusion and discussion

To study QCD phase transitions in different situations are of great importance and it is interesting to consider chiral phase transition at different quark masses. In [5, 63], we proposed a modified soft-wall AdS/QCD model and study chiral phase transition in $N_f = 2$ and $N_f = 3$ case. After extracting temperature dependent chiral condensate, it is found that chiral phase transition is of second order in two flavor chiral limit and turns to be crossover at any finite quark masses, while in three flavor chiral limit it becomes first order and turns to crossover only at sufficient large quark masses. Then, in [65], we have shown that this model can describe inverse magnetic catalysis after considering the Einstein-Maxwell sector. Therefore, in this work, we try to extend these studies to $N_f = 2 + 1$ case when $m_u = m_d \neq m_s$.

The extension of previous study is quite natural and simple. The main different is that the expectation value of the scalar field X in soft-wall model should be taken as 3×3 diagonal matrix $\text{diag}\{\chi_l, \chi_l, \chi_s\}$ other than 2×2 $\text{diag}\{\chi, \chi\}$. If $m_l \neq m_s$, then it is expected that $\chi_l \neq \chi_s$ and one has to deal with the two coupled second order derivative

equations. The UV boundary condition of χ_l, χ_s can be related to quark masses m_l, m_s and chiral condensates σ_l, σ_s . The black hole horizon would come up with another boundary condition, which will require condensates as functions of temperature and quark masses, i.e. of the form $\sigma_l(m_l, m_s, T), \sigma_s(m_l, m_s, T)$.

Fixing m_s and solving the equations of motion, it is found that at both small m_l and large m_l , chiral condensate would decrease from finite value at low temperature to zero at high temperature, indicating a phase transition between symmetry breaking phase at low temperature and symmetry restoration phase at high temperature. Moreover, it is found that at small m_l , σ_l, σ_s are triple valued in certain temperature range, giving the signal of first order phase transition. The triple valued temperature range would decrease with the increasing of m_l , and at certain critical value it disappears and the phase transition become a second order one. If one continues to increase m_l , then σ_l, σ_s will decrease monotonically and the phase transition becomes crossover. Varying m_s , the qualitative behavior is similar. Thus, the whole $m_l - m_s$ plane is divided into two regions: first order region and crossover region as shown in Fig.7(a). The boundary of these two regions is the second order line, which could be extracted by solving critical values of m_l at different m_s . The second order line are divided by the $m_l = m_s$ line into two parts, and it is shown that the m_s dependence of the transition temperature in these two parts are totally contrast, which might indicate that the two parts are governed by different universality classes. Qualitatively, these model results for chiral phase transition in Fig.7 is in agreement with the ‘‘Colombia Plot’’ in Fig.1(a) summarized from lattice simulations and other non-perturbative analysis. It confirms that the soft-wall AdS/QCD framework can provide good holographic description on chiral dynamics.

Acknowledgement

The authors thank Kaddour Chelabi, Zheng Fang, Song He and Yue-Liang Wu for valuable discussions. M.H. is supported by the NSFC under Grant Nos. 11175251 and 11275213, DFG and NSFC (CRC 110), CAS key project KJCX2-EW-N01, and Youth Innovation Promotion Association of CAS. This work is partly supported by China Postdoctoral Science Foundation(2015M580136).

References

- [1] Y. Aoki, G. Endrodi, Z. Fodor, S. D. Katz and K. K. Szabo, ‘‘The Order of the quantum chromodynamics transition predicted by the standard model of particle physics,’’ *Nature* **443** (2006) 675 [hep-lat/0611014].
- [2] E. Laermann and O. Philipsen, ‘‘The Status of lattice QCD at finite temperature,’’ *Ann. Rev. Nucl. Part. Sci.* **53** (2003) 163 [hep-ph/0303042].
- [3] P. de Forcrand and O. Philipsen, ‘‘The Chiral critical line of $N(f) = 2+1$ QCD at zero and non-zero baryon density,’’ *JHEP* **0701** (2007) 077 [hep-lat/0607017].
- [4] K. Kanaya, ‘‘Lattice results on the phase structure and equation of state in QCD at finite temperature,’’ *AIP Conf. Proc.* **1343** (2011) 57 [arXiv:1012.4235 [hep-ph]].

- [5] K. Chelabi, Z. Fang, M. Huang, D. Li and Y. L. Wu, “Chiral Phase Transition in the Soft-Wall Model of AdS/QCD,” *JHEP* **1604**, 036 (2016) [arXiv:1512.06493 [hep-ph]].
- [6] R. D. Pisarski and F. Wilczek, “Remarks on the Chiral Phase Transition in Chromodynamics,” *Phys. Rev. D* **29** (1984) 338.
- [7] J. M. Maldacena, “The large N limit of superconformal field theories and supergravity,” *Adv. Theor. Math. Phys.* **2**, 231 (1998) [*Int. J. Theor. Phys.* **38**, 1113 (1999)] [arXiv:hep-th/9711200].
- [8] S. S. Gubser, I. R. Klebanov and A. M. Polyakov, “Gauge theory correlators from non-critical string theory,” *Phys. Lett. B* **428**, 105 (1998) [arXiv:hep-th/9802109].
- [9] E. Witten, “Anti-de Sitter space and holography,” *Adv. Theor. Math. Phys.* **2**, 253 (1998) [arXiv:hep-th/9802150].
- [10] J. Erlich, E. Katz, D. T. Son, M. A. Stephanov, “QCD and a holographic model of hadrons,” *Phys. Rev. Lett.* **95**, 261602 (2005). [hep-ph/0501128].
- [11] A. Karch, E. Katz, D. T. Son and M. A. Stephanov, “Linear confinement and AdS/QCD,” *Phys. Rev. D* **74** (2006) 015005.
- [12] G. F. de Teramond and S. J. Brodsky, “The hadronic spectrum of a holographic dual of QCD,” *Phys. Rev. Lett.* **94**, 201601 (2005).
- [13] L. Da Rold and A. Pomarol, “Chiral symmetry breaking from five dimensional spaces,” *Nucl. Phys. B* **721**, 79 (2005).
- [14] J. Babington, J. Erdmenger, N. J. Evans, Z. Guralnik and I. Kirsch, “Chiral symmetry breaking and pions in non-supersymmetric gauge/gravity *Phys. Rev. D* **69**, 066007 (2004) [arXiv:hep-th/0306018].
- [15] M. Kruczenski, D. Mateos, R. C. Myers and D. J. Winters, “Towards a holographic dual of large N(c) QCD,” *JHEP* **0405** (2004) 041[hep-th/0311270].
- [16] T. Sakai and S. Sugimoto, “Low energy hadron physics in holographic QCD,” *Prog. Theor. Phys.* **113**, 843 (2005)[arXiv:hep-th/0412141].
- [17] T. Sakai and S. Sugimoto, “More on a holographic dual of QCD,” *Prog. Theor. Phys.* **114**, 1083 (2006). [arXiv:hep-th/0507073].
- [18] C. Csaki and M. Reece, “Toward a systematic holographic QCD: A braneless approach,” *JHEP* **0705**, 062 (2007) [arXiv:hep-ph/0608266].
- [19] S. He, M. Huang, Q. S. Yan and Y. Yang, “Confront Holographic QCD with Regge Trajectories,” *Eur.Phys.J.C.*(2010)66:187. arXiv:0710.0988 [hep-ph].
- [20] T. Gherghetta, J. I. Kapusta and T. M. Kelley, “Chiral symmetry breaking in the soft-wall AdS/QCD model,” *Phys. Rev. D* **79** (2009) 076003;
- [21] T. M. Kelley, S. P. Bartz and J. I. Kapusta, “Pseudoscalar Mass Spectrum in a Soft-Wall Model of AdS/QCD,” *Phys. Rev. D* **83** (2011) 016002;
- [22] Y. -Q. Sui, Y. -L. Wu, Z. -F. Xie and Y. -B. Yang, “Prediction for the Mass Spectra of Resonance Mesons in the Soft-Wall AdS/QCD with a Modified 5D Metric,” *Phys. Rev. D* **81** (2010) 014024;
- [23] Y. -Q. Sui, Y. -L. Wu and Y. -B. Yang, “Predictive AdS/QCD Model for Mass Spectra of Mesons with Three Flavors,” *Phys. Rev. D* **83** (2011) 065030.

- [24] D. Li, M. Huang and Q. S. Yan, “A dynamical soft-wall holographic QCD model for chiral symmetry breaking and linear confinement,” *Eur. Phys. J. C* **73** (2013) 2615 [arXiv:1206.2824 [hep-th]].
- [25] D. Li and M. Huang, “Dynamical holographic QCD model for glueball and light meson spectra,” *JHEP* **1311** (2013) 088 [arXiv:1303.6929 [hep-ph]].
- [26] S. P. Bartz and J. I. Kapusta, “Dynamical three-field AdS/QCD model,” *Phys. Rev. D* **90** (2014) no.7, 074034 [arXiv:1406.3859 [hep-ph]].
- [27] P. Colangelo, F. De Fazio, F. Giannuzzi, F. Jugeau and S. Nicotri, “Light scalar mesons in the soft-wall model of AdS/QCD,” *Phys. Rev. D* **78**, 055009 (2008) [arXiv:0807.1054 [hep-ph]].
- [28] L. Bellantuono, P. Colangelo and F. Giannuzzi, “Holographic Oddballs,” *JHEP* **1510** (2015) 137 [arXiv:1507.07768 [hep-ph]].
- [29] E. Folco Capossoli and H. Boschi-Filho, “Odd spin glueball masses and the Odderon Regge trajectories from the holographic hardwall model,” *Phys. Rev. D* **88** (2013) no.2, 026010 [arXiv:1301.4457 [hep-th]].
- [30] E. Folco Capossoli and H. Boschi-Filho, *Phys. Lett. B* **753** (2016) 419 [arXiv:1510.03372 [hep-ph]].
- [31] E. Folco Capossoli, D. Li and H. Boschi-Filho, “Pomeron and Odderon Regge Trajectories from a Dynamical Holographic Model,” *Phys. Lett. B* **760** (2016) 101 [arXiv:1601.05114 [hep-ph]].
- [32] E. Folco Capossoli, D. Li and H. Boschi-Filho, “Dynamical corrections to the anomalous holographic soft-wall model: the pomeron and the odderon,” *Eur. Phys. J. C* **76** (2016) no.6, 320 [arXiv:1604.01647 [hep-ph]].
- [33] Y. Chen and M. Huang, “Two-Gluon and Trigluon Glueballs from Dynamical Holography QCD,” arXiv:1511.07018 [hep-ph].
- [34] A. Vega and P. Cabrera, “Family of dilatons and metrics for AdS/QCD models,” *Phys. Rev. D* **93** (2016) no.11, 114026 [arXiv:1601.05999 [hep-ph]].
- [35] E. V. Shuryak, “What RHIC experiments and theory tell us about properties of quark-gluon plasma?,” *Nucl. Phys. A* **750**, 64 (2005) [arXiv:hep-ph/0405066].
- [36] M. J. Tannenbaum, “Recent results in relativistic heavy ion collisions: From ’ a new state of Rept. Prog. Phys. **69**, 2005 (2006) [arXiv:nucl-ex/0603003].
- [37] G. Policastro, D. T. Son and A. O. Starinets, “The shear viscosity of strongly coupled $N = 4$ supersymmetric Yang-Mills plasma,” *Phys. Rev. Lett.* **87**, 081601 (2001) [arXiv:hep-th/0104066].
- [38] R. -G. Cai, Z. -Y. Nie, N. Ohta and Y. -W. Sun, “Shear Viscosity from Gauss-Bonnet Gravity with a Dilaton Coupling,” *Phys. Rev. D* **79**, 066004 (2009) [arXiv:0901.1421 [hep-th]].
- [39] R. -G. Cai, Z. -Y. Nie and Y. -W. Sun, “Shear Viscosity from Effective Couplings of Gravitons,” *Phys. Rev. D* **78**, 126007 (2008) [arXiv:0811.1665 [hep-th]].
- [40] S. J. Sin and I. Zahed, “Holography of radiation and jet quenching,” *Phys. Lett. B* **608**, 265 (2005) [arXiv:hep-th/0407215];
- [41] E. Shuryak, S. J. Sin and I. Zahed, “A Gravity Dual of RHIC Collisions,” *J. Korean Phys. Soc.* **50**, 384 (2007) [arXiv:hep-th/0511199].

- [42] H. Nastase, “The RHIC fireball as a dual black hole,” arXiv:hep-th/0501068.
- [43] R. A. Janik and R. B. Peschanski, “Asymptotic perfect fluid dynamics as a consequence of AdS/CFT,” Phys. Rev. D **73**, 045013 (2006) [arXiv:hep-th/0512162];
- [44] S. Nakamura and S. J. Sin, “A holographic dual of hydrodynamics,” JHEP **0609**, 020 (2006) [arXiv:hep-th/0607123];
- [45] S. J. Sin, S. Nakamura and S. P. Kim, “Elliptic Flow, Kasner Universe and Holographic Dual of RHIC Fireball,” JHEP **0612**, 075 (2006) [arXiv:hep-th/0610113].
- [46] C. P. Herzog, A. Karch, P. Kovtun, C. Kozcaz and L. G. Yaffe, “Energy loss of a heavy quark moving through $N = 4$ supersymmetric Yang-Mills plasma,” JHEP **0607**, 013 (2006) [arXiv:hep-th/0605158]
- [47] S. S. Gubser, “Drag force in AdS/CFT,” Phys. Rev. D **74**, 126005 (2006) [arXiv:hep-th/0605182].
- [48] Y. Wu, D. Hou and H. c. Ren, “Some Comments on the Holographic Heavy Quark Potential in a Thermal Bath,” arXiv:1401.3635 [hep-ph].
- [49] D. Li, S. He and M. Huang, “Temperature dependent transport coefficients in a dynamical holographic QCD model,” JHEP **1506** (2015) 046 [arXiv:1411.5332 [hep-ph]].
- [50] D. Li, J. Liao and M. Huang, “Enhancement of jet quenching around phase transition: result from the dynamical holographic model,” Phys. Rev. D **89** (2014) 12, 126006 [arXiv:1401.2035 [hep-ph]].
- [51] O. Aharony, S. S. Gubser, J. M. Maldacena, H. Ooguri and Y. Oz, “Large N field theories, string theory and gravity,” Phys. Rept. **323**, 183 (2000) [arXiv:hep-th/9905111].
- [52] J. Erdmenger, N. Evans, I. Kirsch and E. Threlfall, “Mesons in Gauge/Gravity Duals - A Review,” Eur. Phys. J. A **35** (2008) 81 [arXiv:0711.4467 [hep-th]].
- [53] G. F. de Teramond and S. J. Brodsky, “Hadronic Form Factor Models and Spectroscopy Within the Gauge/Gravity Correspondence,” arXiv:1203.4025 [hep-ph].
- [54] Y. Kim, I. J. Shin and T. Tsukioka, “Holographic QCD: Past, Present, and Future,” Prog. Part. Nucl. Phys. **68** (2013) 55 [arXiv:1205.4852 [hep-ph]].
- [55] A. Adams, L. D. Carr, T. Schfer, P. Steinberg and J. E. Thomas, “Strongly Correlated Quantum Fluids: Ultracold Quantum Gases, Quantum Chromodynamic Plasmas, and Holographic Duality,” New J. Phys. **14** (2012) 115009 [arXiv:1205.5180 [hep-th]].
- [56] I. Iatrakis, E. Kiritsis and A. Paredes, “An AdS/QCD model from tachyon condensation: II,” JHEP **1011** (2010) 123 [arXiv:1010.1364 [hep-ph]].
- [57] M. Jarvinen and E. Kiritsis, “Holographic Models for QCD in the Veneziano Limit,” JHEP **1203** (2012) 002 [arXiv:1112.1261 [hep-ph]].
- [58] T. Alho, M. Jarvinen, K. Kajantie, E. Kiritsis and K. Tuominen, “On finite-temperature holographic QCD in the Veneziano limit,” JHEP **1301** (2013) 093 [arXiv:1210.4516 [hep-ph]].
- [59] P. Colangelo, F. Giannuzzi, S. Nicotri and V. Tangorra, “Temperature and quark density effects on the chiral condensate: An AdS/QCD study,” Eur. Phys. J. C **72** (2012) 2096 [arXiv:1112.4402 [hep-ph]].
- [60] N. Evans, C. Miller and M. Scott, “Inverse Magnetic Catalysis in Bottom-Up Holographic QCD,” arXiv:1604.06307 [hep-ph].

- [61] D. Dudal, D. R. Granado and T. G. Mertens, “No inverse magnetic catalysis in the QCD hard and soft wall models,” *Phys. Rev. D* **93**, no. 12, 125004 (2016) [arXiv:1511.04042 [hep-th]].
- [62] S. P. Bartz and T. Jacobson, “Chiral Phase Transition and Meson Melting from AdS/QCD,” arXiv:1607.05751 [hep-ph].
- [63] K. Chelabi, Z. Fang, M. Huang, D. Li and Y. L. Wu, “Realization of chiral symmetry breaking and restoration in holographic QCD,” *Phys. Rev. D* **93**, no. 10, 101901 (2016) [arXiv:1511.02721 [hep-ph]].
- [64] Z. Fang, S. He and D. Li, “Chiral and Deconfining Phase Transitions from Holographic QCD Study,” *Nucl. Phys. B* **907** (2016) 187 [arXiv:1512.04062 [hep-ph]].
- [65] D. Li, M. Huang, Y. Yang and P. H. Yuan, “Inverse Magnetic Catalysis in the Soft-Wall Model of AdS/QCD,” arXiv:1610.04618 [hep-th].
- [66] G. S. Bali, F. Bruckmann, G. Endrodi, Z. Fodor, S. D. Katz, S. Krieg, A. Schafer and K. K. Szabo, “The QCD phase diagram for external magnetic fields,” *JHEP* **1202**, 044 (2012) [arXiv:1111.4956 [hep-lat]].
- [67] G. S. Bali, F. Bruckmann, G. Endrodi, Z. Fodor, S. D. Katz and A. Schafer, “QCD quark condensate in external magnetic fields,” *Phys. Rev. D* **86**, 071502 (2012) [arXiv:1206.4205 [hep-lat]].
- [68] K. Fukushima and Y. Hidaka, “Magnetic Catalysis vs Magnetic Inhibition,” *Phys. Rev. Lett.* **110**, 031601 (2013) [arXiv:1209.1319 [hep-ph]].
- [69] T. Kojo and N. Su, “The quark mass gap in a magnetic field,” *Phys. Lett. B* **720**, 192 (2013) [arXiv:1211.7318 [hep-ph]].
- [70] F. Bruckmann, G. Endrodi and T. G. Kovacs, “Inverse magnetic catalysis and the Polyakov loop,” *JHEP* **1304**, 112 (2013) [arXiv:1303.3972 [hep-lat]].
- [71] J. Chao, P. Chu and M. Huang, “Inverse magnetic catalysis induced by sphalerons,” *Phys. Rev. D* **88**, 054009 (2013) [arXiv:1305.1100 [hep-ph]].
- [72] E. S. Fraga, B. W. Mintz and J. Schaffner-Bielich, “A search for inverse magnetic catalysis in thermal quark-meson models,” *Phys. Lett. B* **731**, 154 (2014) [arXiv:1311.3964 [hep-ph]].
- [73] M. Ferreira, P. Costa, O. Lourenco, T. Frederico and C. Providencia, “Inverse magnetic catalysis in the (2+1)-flavor Nambu–Jona-Lasinio and Polyakov–Nambu–Jona-Lasinio models,” *Phys. Rev. D* **89**, 116011 (2014) [arXiv:1404.5577 [hep-ph]].
- [74] R. L. S. Farias, K. P. Gomes, G. I. Krein and M. B. Pinto, “Importance of asymptotic freedom for the pseudocritical temperature in magnetized quark matter,” *Phys. Rev. C* **90**, no. 2, 025203 (2014) [arXiv:1404.3931 [hep-ph]].
- [75] L. Yu, H. Liu and M. Huang, “Spontaneous generation of local CP violation and inverse magnetic catalysis,” *Phys. Rev. D* **90**, 074009 (2014) [arXiv:1404.6969 [hep-ph]].
- [76] J. O. Andersen, W. R. Naylor and A. Tranberg, “Inverse magnetic catalysis and regularization in the quark-meson model,” arXiv:1410.5247 [hep-ph].
- [77] E. J. Ferrer, V. de la Incera and X. J. Wen, “Quark Antiscreening at Strong Magnetic Field and Inverse Magnetic Catalysis,” arXiv:1407.3503 [nucl-th].
- [78] B. Feng, D. Hou and H. c. Ren, “(Inverse) Magnetic Catalysis in Bose-Einstein Condensation of Neutral Bound Pairs,” arXiv:1412.1647 [cond-mat.quant-gas].

- [79] A. Cherman, T. D. Cohen and E. S. Werbos, “The Chiral condensate in holographic models of QCD,” *Phys. Rev. C* **79** (2009) 045203 [arXiv:0804.1096 [hep-ph]].